IET Generation, Transmission & Distribution

Research Article

IET Journals
The Institution of Engineering and Technology

Developed generalised unified power flow controller model in the Newton–Raphson power-flow analysis using combined mismatches method

ISSN 1751-8687
Received on 14th October 2015
Revised on 3rd December 2015
Accepted on 2nd February 2016
doi: 10.1049/iet-gtd.2015.1247
www.ietdl.org

Salah Kamel[1] ✉, *Francisco Jurado*[2], *Zhe Chen*[3], *Mamdouh Abdel-Akher*[1,4], *Mohamed Ebeed*[5]

[1]*Electrical Engineering Department, Aswan Faculty of Engineering, Aswan University, 81542 Aswan, Egypt*
[2]*Department of Electrical Engineering, University of Jaén, 23700 EPS Linares, Jaén, Spain*
[3]*Department of Energy Technology, Aalborg University, Aalborg, 9220, Denmark*
[4]*Electrical Engineering Department, College of Engineering, Qassim University, King Abdulaziz Road, Unaizah 56434, Qassim, Kingdom of Saudi Arabia*
[5]*Egyptian Ferro Silicon Alloys Company, Aswan, Egypt*
✉ *E-mail: skamel@aswu.edu.eg*

Abstract: This study proposes the generalised unified power flow controller (GUPFC) model in the hybrid current power mismatch Newton–Raphson formulation (HPCIM). In this model, active power, real and imaginary current components are injected at the terminals of series impedances of GUPFC. These injected values are calculated during the iterative process based on the desired controlled values and buses voltage at the terminals of GUPFC. The parameters of GUPFC can be calculated during the iterative process and the final values are updated after load flow convergence. Using the developed GUPFC model, the original structure and symmetry of the admittance and Jacobian matrices can still be kept, the changing of Jacobian matrix is eliminated. Consequently, the complexities of the computer load flow program codes with GUPFC are reduced. The HPCIM load flow code with the proposed model is written in C++ programming language. Where, the SuperLU library is utilised to handle the sparse Jacobian matrix. The proposed model has been validated using the standard IEEE test systems.

Nomenclature

FACTS	flexible AC transmission system
IPFC	interline power flow controller
STATCOM	static synchronous compensator
UPFC	unified power-flow controller
GTO	gate turn-off
PIM	power injection mismatch
CIM	current injection mismatch
HPCIM	hybrid power/current injection mismatches
p.u.	per unit
NR	Newton–Raphson method
PV	voltage controlled buses
PQ	load buses
N	total number of buses
T	iterations counter
P, Q	active and reactive complex powers
$\Delta I_{xr} + \mathrm{j}\Delta I_{xm}$	complex current mismatch at bus x
$\Delta V_{xr} + \mathrm{j}\Delta V_{xm}$	complex voltage mismatch at bus x
ΔP_y	active power mismatch at bus y
r, m	subscripts refer to real and imaginary parts
i, j, k, h	subscripts refer to nodes
Sp	superscript refers to specified values
Cal	superscript refers to calculated values
Inj	subscripts refer to injected value
se, sh	subscripts refer to series and shunt converters
$\boldsymbol{G}$, $\boldsymbol{B}$	elements of nodal admittance matrix
Q_k^{L}	reactive power consumed by load at bus k

1 Introduction

Nowadays power systems are operated close to their limits due to geographical, environmental constraints, or high initial investment cost. Flexible AC transmission system (FACTS) devices are considered the key technology that promoted to increase power systems capabilities through many active and reactive powers control options. The integration of FACTS increases the controllability and enhances the power transfer capability of existing transmission network infrastructure [1]. The analysis of sophisticated and congested power systems requires efficient and robust power-flow methods. The primary requirement of a power-flow method is the ability to accommodate for various new power system devices, including FACTS, without degrading the performance or losing solution accuracy [1–3]. Consequently, power-flow methods have been always subject to extensive research over the years to improve the performance or integrate new technologies. Over the last decades, the Newton–Raphson (NR) method is considered the most reliable power-flow solver which has been adopted to simulate and analyse interconnected power systems [3]. To improve its performance, the NR method involved many variants and simplifications [4–6]. The so-called variant of the full NR is the fast decupled (FD) method. This method has found widespread usage in industry due its superior performance [4]. However, due to the complexity of the FACTS modelling, the majority of FACTS implementation achieved using the full NR formulation [1, 2].

FACTS devices are basically classified into two main generations: the first utilises conventional thyristor whereas the second generation employs the gate turn-off thyristors [1, 2]. The later generation allows more control options utilising voltage source converters. In [7], the unified power-flow controller (UPFC) capabilities in multiple lines compensation have been integrated into a generalised power-flow controller. A framework for steady-state and dynamic models then has been formulated and verified [8]. In line with UPFC modelling, other FACTS devices such as static series synchronous compensator (SSSC) and interline power flow controller (IPFC) devices have been proposed [9, 10]. The integration of UPFC in the power-flow analysis is then presented [11–13]. Steady-state UPFC models have been developed and

validated in NR power-flow for analysing large networks [11]. To control the UPFC parameters simultaneously, the UPFC state variables are embedded inside the Jacobian and mismatch equations [12, 13]. The IPFC and GUPFC are included the NR Jacobian matrix to improve the convergence rate [14].

The complexity of NR implementation with FACTS has been subject to investigation to make codes reusable and less independent on the original Jacobian matrix [15–17]. The matrix partitioning approach has been applied to model UPFC in NR load flow algorithm [15], which still requires a special code to be solved with the Jacobian matrix. The indirect approach for implementing FACTS in NR power-flow analysis increases the size of the Jacobian matrix to represent the additional state variables of FACTS [16, 17]. Also, determination of the operating constraints of FACTS controllers is considered an important issue to realise the practical capabilities of these devices. The operating constraints of FACTS depend upon their converters rating. The authors [18–21] have presented some FACTS devices and developed methods for handling their violated limits.

The current injection mismatch (CIM) is a typical NR approach that utilises current mismatches instead of power mismatches in formulation the problem [5]. This method has been particularly intended to retain the same convergence character of original solver with execution time 70% faster [22]. The inadequacy associated with the CIM excellent performance is the implementation of voltage control nodes. Consequently, CIM method has found wide application in distribution system analysis [22, 23]. The voltage control nodes have been subsequently solved by augmentation of NR Jacobian matrix. This leads to an even larger size of NR Jacobian matrix according to the number of voltage control nodes [6, 24]. A new approach for handling voltage control nodes has been proposed using HPCIM formulation [21, 25]. This technique ensures same problem size of Jacobian matrix, keeps convergence rate of NR, and finally guarantees fast execution time [25–27]. The HPCIM method keeps the NR convergence character with superior performance providing very efficient power solver for FACTS integration [28–32]. These successful implementations of various FACTS in HPCIM power-flow inspire the authors to formulate and develop the GUPFC model in this paper.

The GUPFC consists of a hybrid between series and shunt controllers to regulate the multi-line power flow and voltage bus individually or simultaneously [14, 33]. The implementation of GUPFC into power-flow solution is considered a fundamental requirement for power system operation planning and control studies. A few publications have been focused on the mathematical modelling of GUPFC in power-flow analysis [14]. Based on these publications, new Jacobian subblocks have to be formulated which alters the basic load-flow codes. In this paper, the GUPFC is modelled and incorporated in HPCIM power-flow without any limitation on voltage control nodes [25]. The original structure and symmetry of admittance and Jacobian matrices are not changed. The only requirement is the mismatch vector at the terminal buses of GUPFC. Consequentially, the complexity of load flow codes with GUPFC is effectively decreased. The GUPFC parameters are calculated during the iterative process, where, the final values of these parameters are updated after HPCIM power-flow convergence. The developed model overcomes the problem that happens when the GUPFC is the only link between two sub-networks [8]. This paper presents results of computer simulations showing the performance of GUPFC under different system conditions.

2 HPCIM formulation

A new formulation has been developed to provide a better modelling of voltage controlled devices in the CIM method [25–27]. This approach has been adopted in the current work to model the GUPFC as will be discussed in the following section. A combination between NR formulation based on power injection mismatches (PIMs) and CIM formulation have been developed. In this new methodology, PQ nodes are expressed using CIM based on real and imaginary parts of injected currents at these nodes. On the other hand, PV nodes are represented using PIM based on the real power mismatches. The HPCIM formulation can be expressed as follows

$$\begin{bmatrix} \Delta \boldsymbol{I}_{xm} \\ \Delta \boldsymbol{I}_{xr} \\ \Delta \boldsymbol{P}_{y} \end{bmatrix} = \begin{bmatrix} & & \dfrac{\partial \boldsymbol{I}_{m}}{\partial \boldsymbol{\delta}} \\ & \boldsymbol{J}_{x} & \dfrac{\partial \boldsymbol{I}_{xr}}{\partial \boldsymbol{\delta}} \\ \dfrac{\partial \boldsymbol{P}_{y}}{\partial \boldsymbol{V}} & \dfrac{\partial \boldsymbol{P}_{y}}{\partial \boldsymbol{V}} & \dfrac{\partial \boldsymbol{P}_{y}}{\partial \boldsymbol{\delta}} \end{bmatrix} \begin{bmatrix} \Delta \boldsymbol{V}_{xr} \\ \Delta \boldsymbol{V}_{xm} \\ \Delta \boldsymbol{\delta}_{y} \end{bmatrix} \quad \begin{matrix} x \in PQ \text{ nodes} \\ y \in PV \text{ nodes} \end{matrix} \tag{1}$$

where the sub-block $\boldsymbol{J}_x$ corresponds to the CIM Jacobian matrix [5]. The current mismatch equations are calculated for PQ nodes as follows

$$\Delta I_{rx} = \frac{P_k^{\text{sp}} V_{rx} + Q_k^{\text{sp}} V_{mx}}{V_{rx}^2 + V_{mx}^2} - \sum_{i=1}^{n} (G_{xi} V_{ri} - B_{xi} V_{mi}) \tag{2}$$

$$\Delta I_{mx} = \frac{P_x^{\text{sp}} V_{mx} + Q_k^{\text{sp}} V_{rx}}{V_{rx}^2 + V_{mx}^2} - \sum_{i=1}^{n} (G_{xi} V_{mi} - B_{xi} V_{ri}) \tag{3}$$

The bus voltages are updated during the iterative process as real and imaginary components as follows

$$V_{rx}^{t+1} = V_{rx}^{t} + \Delta V_{rx}^{t} \tag{4}$$

$$V_{mx}^{t+1} = V_{mx}^{t} + \Delta V_{mx}^{t} \tag{5}$$

$$\left|V_x^{t+1}\right| = \sqrt{\left(V_{mx}^{t}\right)^2 + \left(\Delta V_{mx}^{t}\right)^2} \tag{6}$$

$$\delta_x^{t+1} = \tan^{-1}\left(\frac{V_{mx}^{t}}{V_{rx}^{t}}\right) \tag{7}$$

The interesting in (1) that each PV node is expressed by a single equation instead of three equations in the classical CIM formulation [5, 6, 24]. The real power mismatches representation of a certain PV bus, say bus 'f' is expressed as follows

$$\Delta P_f = P_f^{\text{sp}} - \sum_{i=1}^{N} \left|V_f\right| \left|V_i\right| (G_{fi} \cos \delta_{fi} + B_{fi} \sin \delta_{fi}) \tag{8}$$

The corresponding derivatives of the PV nodes in the Jacobian matrix are given in [25, 26]. The bus angle is updated as follows

$$\delta_f^{t+1} = \delta_f^{t} + \Delta \delta_f^{t} \tag{9}$$

3 Implementation of the GUPFC model

The GUPFC mathematical model consists of one shunt converter and two or more series converters. The real power is exchanged among these shunt and series converters via a common dc link. The sum of active power exchanged must equal to zero if the switching losses of the converter circuits are neglected [1, 14, 33].

The GUPFC schematic diagram consists of three converters. These converters are connected via common dc link as shown in Fig. 1. In steady state operation, this simplest GUPFC controller can be represented by two voltage sources (V_1^{se} and V_2^{se}) representing the output voltage of two series converters and one controllable shunt injected voltage source (V^{sh}). Where, the connected impedances represent the leakage reactance of the coupling transformers (Z_1^{se}, Z_2^{se} and Z^{sh}). According to the equivalent circuit of GUPFC in Fig. 2*a*, the developed GUPFC model can be represented by a combined power and current injection approach as given in Fig. 2*b*.

During the iteration process of the load flow algorithm, active power and currents are injected at terminals of GUPFC (sending and auxiliary buses). These injected values are calculated using the voltage of terminal buses, pre-specified line flows and the required

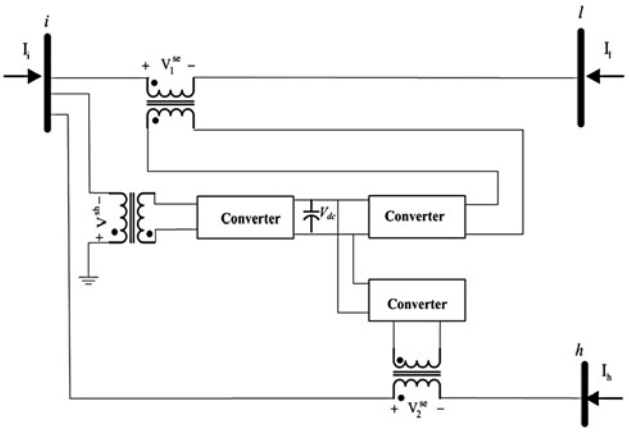

Fig. 1 *Schematic diagram of three converters GUPFC controller*

voltage at shunt bus. The control parameters of this device can be updated using new buses voltage and these injected power and currents at the terminals of GUPFC. Using this representation of GUPFC device, the control of active, reactive power and voltage can be performed simultaneously or individually, the problem when GUPFC is the only link between two sub networks is eliminated. Moreover, the model enhances the reusability for load flow code by avoiding HPCIM power-flow Jacobian modification. The mathematical model of the GUPFC is represented in the following subsections.

3.1. Model of GUPFC series compensators

3.1.1 Representation of GUPFC series compensator of line # 1: Both the active and reactive power flows are controlled, hence, the transmitted current between the first auxiliary bus i and the first receiving bus h is specified and the shunt injected current at bus i can be calculated as

$$I_1^{\text{Inj}} = \left(\frac{P_{ih}^{\text{sp}} + \text{j}Q_{ih}^{\text{sp}}}{V_i}\right)^* - \left(\frac{V_k - V_i}{Z_1^{\text{se}}}\right) \tag{10}$$

By substituting the real and imaginary components of the voltages, series impedance and specified power in (10), the real and imaginary components of this shunt injected current can be given by the following equations

$$I_{r1}^{\text{Inj}} = \frac{P_1^{\text{sp}} V_{ir} + Q_1^{\text{sp}} V_{im}}{V_i^2} - \frac{\left(R_1^{\text{se}}\left(V_{kr} - V_{ir}\right) + X_1^{\text{se}}\left(V_{km} - V_{im}\right)\right)}{\left(Z_1^{\text{se}}\right)^2} \tag{11}$$

$$I_{m1}^{\text{Inj}} = \frac{P_1^{\text{sp}} V_{im} - Q_1^{\text{sp}} V_{ir}}{V_i^2} - \frac{\left(R_1^{\text{se}}\left(V_{km} - V_{im}\right) - X_1^{\text{se}}\left(V_{kr} - V_{ir}\right)\right)}{\left(Z_1^{\text{se}}\right)^2} \tag{12}$$

These two components of the shunt current are injected at the first auxiliary bus and also at the sending bus as active load with opposite sign, if this bus is assumed voltage control type, as shown in Fig. 3*a*.

3.1.2 Representation of GUPFC series compensator of line # 2: The only active power flow is controlled and the reactive power flow between the second auxiliary and receiving buses should be calculated depending on the system. In this case, the shunt injected current at bus j can be calculated as follows

$$I_2^{\text{Inj}} = \left(\frac{P_{jl}^{\text{sp}} + \text{j}Q_{jl}}{V_j}\right)^* - \left(\frac{V_k - V_j}{Z_2^{\text{se}}}\right) \tag{13}$$

The uncontrolled reactive power flow between the second auxiliary and receive buses Q_{jl} can be calculated as

$$Q_{jl} = \text{Im}\left(V_j I_{jl}^*\right) \tag{14}$$

$$I_{jl} = j\left(\frac{B}{2}\right)V_j + Y_{jl}\left(V_j - V_l\right) \tag{15}$$

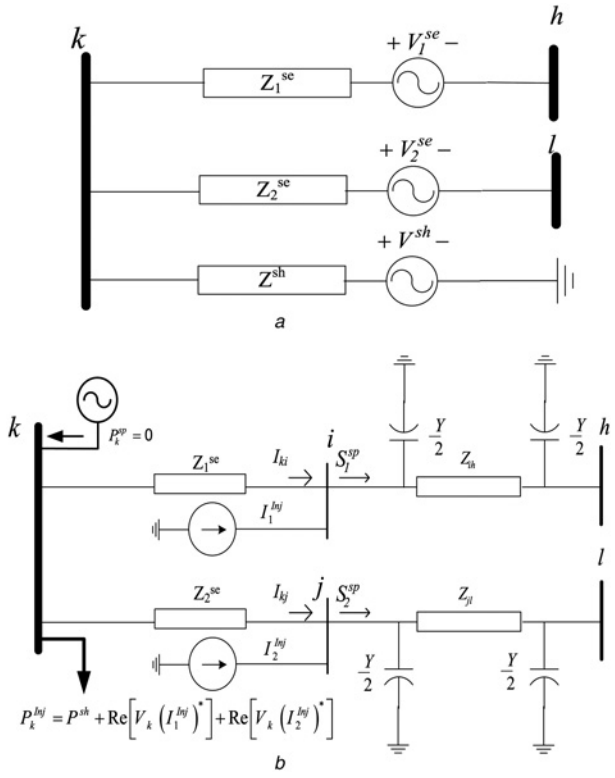

Fig. 2 *Combined power and current injection GUPFC model*
a Equivalent circuit of GUPFC
b Developed GUPFC model

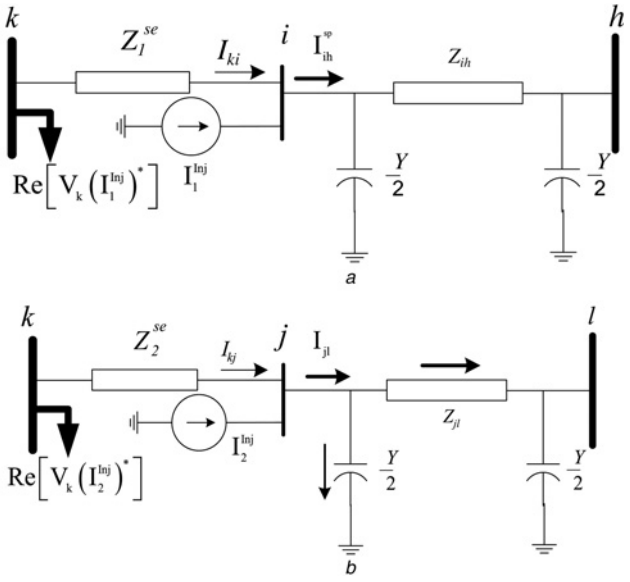

Fig. 3 *GUPFC series representation*
a First line of GUPFC
b Second line of GUPFC

Consequently, the Q_{jl} can be given by

$$Q_{jl} = V_{jm}\left(G_{jl}\left(V_{jr} - V_{lr}\right) - B_{jl}\left(V_{jm} - V_{lm}\right) - V_{jm}\left(\frac{B}{2}\right)\right) - V_{jr}\left(G_{jl}\left(V_{jm} - V_{lm}\right) + B_{il}\left(V_{ir} - V_{lr}\right) + V_{lr}\left(\frac{B}{2}\right)\right) \quad (16)$$

The injected shunt current at bus j can be calculated as a function of the specified active power flow, the reactive power flow between second auxiliary and receiving buses and the voltage values at the terminals of GUPFC model in the second line as presented in the following equations

$$I_{r2}^{\text{Inj}} = \frac{P_2^{\text{sp}} V_{jr} + Q_{jl} V_{jm}}{V_j^2} - \frac{\left(R_2^{\text{se}}\left(V_{kr} - V_{jr}\right) + X_2^{\text{se}}\left(V_{km} - V_{jm}\right)\right)}{\left(Z_2^{\text{se}}\right)^2} \quad (17)$$

$$I_{m2}^{\text{Inj}} = \frac{P_2^{\text{sp}} V_{jm} - Q_{jl} V_{jr}}{V_j^2} - \frac{\left(R_2^{\text{se}}\left(V_{km} - V_{jm}\right) - X_2^{\text{se}}\left(V_{kr} - V_{jr}\right)\right)}{\left(Z_2^{\text{se}}\right)^2} \quad (18)$$

The above real and imaginary components of shunt current are injected at the second auxiliary bus and also at the sending bus as active load with opposite sign, as shown in Fig. 3*b*.

3.2 Representation of GUPFC shunt compensator

The shunt converter equivalent circuit of GUPFC is shown separately in Fig. 4*a*. This shunt converter supplies a complex power ($S_{\text{sh}} = P_{\text{sh}} + \text{j}Q_{\text{sh}}$) to the system at connected bus k.

The shunt converter can be represented as an asynchronous condenser, hence, the connected bus is converted to PV bus with the specified voltage value and reactive power Q^{sh}, which is used to maintain the required voltage magnitude at bus k as shown in Fig. 4*b*. The Q^{sh} can be calculated using the following equation

$$Q_k^{\text{sh}} = \sum_{i=1}^{N} |V_k||V_i|\left(G_{k,i}\sin\delta_{k,i} - B_{k,i}\cos\delta_{k,i}\right) + Q_k^{\text{L}} \quad (19)$$

The active power P^{sh} of this converter is represented as a load at bus k as shown in Fig. 2*b*, where the value of this injected load can be calculated using the basic principle of the active power balance of GUPFC as given in the following equation

$$P_k^{\text{sh}} = -\left(P_1^{\text{se}} + P_2^{\text{se}}\right) \quad (20)$$

where P_1^{se} and P_2^{se} can be calculated as follows

Based on the following equation

$$\left(\frac{S_1^{\text{sp}}}{V_k}\right)^* = \left(\frac{V_{i+V_1^{\text{se}}-V_k}}{Z_1^{\text{se}}}\right) \quad (21)$$

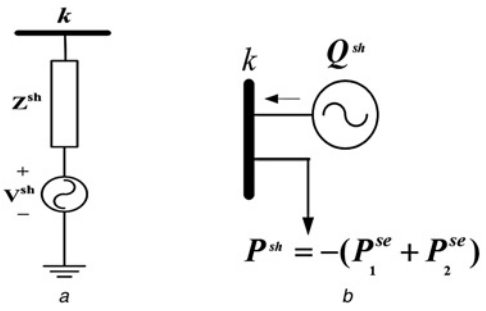

Fig. 4 *Model of GUPFC shunt compensator*

a Equivalent circuit

b Condenser representation

The P_1^{se} can be given by

$$P_1^{\text{se}} = \frac{V_1^{rse}}{\left(Z_2^{\text{se}}\right)^2}\left(R_1^{\text{se}}\left(V_{ri} + V_1^{rse} - V_{rk}\right) + X_1^{\text{se}}\left(V_{mi} + V_1^{mse} - V_{mk}\right)\right) + \frac{V_1^{mse}}{\left(Z_1^{\text{se}}\right)^2}\left(-R_1^{\text{se}}\left(V_{mi} + V_1^{mse} - V_{mk}\right) + X_1^{\text{se}}\left(V_{ri} + V_1^{rse} - V_{rk}\right)\right) \quad (22)$$

Similarly

$$\left(\frac{S_2^{\text{sp}}}{V_k}\right)^* = \left(\frac{V_{j+V_2^{\text{se}}-V_k}}{Z_2^{\text{se}}}\right) \quad (23)$$

The P_2^{se} can be given by

$$P_2^{\text{se}} = \frac{V_2^{rse}}{\left(Z_2^{\text{se}}\right)^2}\left(R_2^{\text{se}}\left(V_{ri} + V_2^{rse} - V_{rk}\right) + X_2^{\text{se}}\left(V_{mi} + V_2^{mse} - V_{mk}\right)\right) + \frac{V_1^{mse}}{\left(Z_2^{\text{se}}\right)^2}\left(-R_2^{\text{se}}\left(V_{mi} + V_2^{mse} - V_{mk}\right) + X_2^{\text{se}}\left(V_{ri} + V_2^{rse} - V_{rk}\right)\right) \quad (24)$$

3.3 Evaluating the GUPFC parameters

The parameters of the first series compensator can be calculated using the following equation

$$V_1^{\text{se}} = I_1^{\text{Inj}} Z_1^{\text{se}} \quad (25)$$

The parameters of the second series compensator can be calculated using the following equation

$$V_2^{\text{se}} = I_2^{\text{Inj}} Z_2^{\text{se}} \quad (26)$$

Using Kirchhoff's voltage law, the shunt compensator voltage can be calculated using the following equation

$$V^{\text{sh}} = V_k + Z^{\text{sh}}\left(\frac{P_k^{\text{sh}} + \text{j}Q_k^{\text{sh}}}{V_k}\right)^* \quad (27)$$

The real and imaginary components of V_1^{se}, V_2^{se} and V^{sh} are updated during the iterative process and the final values calculated after the convergence of the load flow.

4 Overall solution process

Based on the above developed model, the incorporating of GUPFC into new HPCIM power flow method is discussed in this section. Without altering the basic code of the HPCIM method, the mismatches at the terminals of GUPFC are updated according to the new injected active power at sending buses and currents at the auxiliary buses and the overall solution process can be summarised in the following steps:

Step 1: Modify the system data to handle the new dummy nodes, lines and impedances that represent the GUPFC device.

Step 2: Calculate the power and current mismatches using (2), (3) and (8). At the GUPFC buses, the corresponding injected power and currents should be included in the mismatch equations. The current injections are updated using equations include (11) and (12) for line # 1 and (17) and (18) for line # 2. On the other hand, the power injection is updated using (20) for the shunt branch. Consequently, the final mismatch equations for the GUPFC buses

become as follows

$$\Delta I_{mi} = I_{mi}^{\text{sp}} - I_{mi}^{\text{cal}} + I_{r1}^{\text{Inj}} \quad (28)$$

$$\Delta I_{ri} = I_{ri}^{\text{sp}} - I_{ri}^{\text{cal}} + I_{r1}^{\text{Inj}} \quad (29)$$

$$\Delta I_{mj} = I_{mj}^{\text{sp}} - I_{mj}^{\text{cal}} + I_{m2}^{\text{Inj}} \quad (30)$$

$$\Delta I_{rj} = I_{rj}^{\text{sp}} - I_{rj}^{\text{cal}} + I_{r2}^{\text{Inj}} \quad (31)$$

$$\Delta P_k = P_k^{\text{sp}} - P_k^{\text{cal}} - P_k^{\text{sh}} \quad (32)$$

Step 3: Solve the HPCIM power flow, it is important herein to mention that a public domain, called SuperLU [34], has been utilised to handle the sparse Jacobian matrix.
Step 4: Update the parameters of GUPFC during each iterative process.
Step 5: Check the convergence of power flow problem, otherwise proceed to Step 2.
Step 6: Compute the final solution of GUPFC using (25)–(27) and the power flow solution with necessary details.

The operating constraints are handled by changing the primary controlled set points of GUPFC controller to be within their limits. There are five operating constraints of GUPFC that are checked and handled in the developed GUPFC model; the injected voltage of series and shunt converters (V_1^{se}, V_2^{se}, V^{sh}) and the injected currents passing through the series converters (I_{ih}^{sp}, I_{jl}^{sp}). However, these constraints can be handled as follows:

- If V_1^{se} is violated, it can be enforced by reducing P_1^{sp} gradually to zero and the value of Q_1^{sp} is kept constant until V_{se1} equals to $V_{\max}^{\text{se1}}$. However, if the value of series current still violated; the value of P_1^{sp} is kept at zero and Q_1^{sp} is released until V_1^{se} equals to $V_{\max}^{\text{se1}}$.
- If V_2^{se} is violated, it can be enforced by the same way of handling V_{se1} by releasing P_2^{sp} and Q_2^{sp} instead of P_1^{sp} and Q_1^{sp} until V_2^{se} equals to $V_{\max}^{\text{se2}}$.
- If V^{sh} is violated, it can be enforced by relaxing the specified voltage (V^{sp}) until V^{sh} equals to $V_{\max}^{\text{sh}}$.
- If I_{ih}^{sp} is violated, it can be enforced by reducing P_1^{sp} gradually to zero and the value of Q_{sp1} is kept constant until I_{ih}^{sp} equals to $I_{ih\_\max}^{\text{sp}}$. However, if the value of series current still violated, the value of P_1^{sp} is kept at zero and Q_1^{sp} is released until I_{ih}^{sp} equals to $I_{ih\_\max}^{\text{sp}}$. Note, this current is considered violated value if its value is more than rated value of GUPFC series converter or more than thermal limit of the transmission line.
- If I_{jl}^{sp} is violated, it can be enforced by the same way of handling I_{ih}^{sp} by releasing P_2^{sp} and Q_2^{sp} instead of P_1^{sp} and Q_1^{sp} until I_{jl}^{sp} equals to $I_{jl\_\max}^{\text{sp}}$.

5 Results and discussions

The developed GUPFC model in new HPCIM load flow method is validated using the standard IEEE test system. The test systems are chosen to show the capabilities of the proposed GUPFC model in small- and large-scale power networks. In all case studies, the convergence tolerances are taken equal to 10^{-5} and system base MVA is 100. Load flow codes with the developed GUPFC model have been written using C++ programming language, where, the SuperLU library has been used to perform the calculation of all matrices associated with the power flow solution process. The convergence characteristics and the average computation time per iteration of NR and HPCIM load flow methods are investigated and presented in Table 1. It can be observed that the HPCIM method keeps the NR convergence character and ensures the same size of Jacobian. At the same time, the average computation time per iteration for HPCIM is less than the conventional NR.

Table 1 Average execution time per iteration: NR and HPCIM load flow methods at tolerance = 0.001

IEEE system	NR		HPCIM	
	No. of iterations	Time per iteration, s	No. of iterations	Time per iteration, s
IEEE 5	2	–	2	–
IEEE 30	3	0.0085	3	0.0038
IEEE 118	3	0.0258	3	0.0100

5.1 Test case I

This system consists of four loads totalling 165 MW. It has two generators with seven branches. This system is connected to a slack bus generator at bus 1. The data of this system is available in [12]. The main objective for this test is to validate the developed GUPFC model into HPCIM load flow method. The system is modified by placing a GUPFC on lines 4-3 and 4-5, as shown in Fig. 5.

New auxiliary buses 6 and 7 are added to the system as reference buses. The leakage reactance of the series and shunt coupling transformers of the GUPFC is considered as 0.1 p.u. The purpose of adding the GUPFC on this network is to maintain the active and reactive powers leaving GUPFC towards buses 3 and 5 to be 50 MW, 5 MVAR and 40 MW, respectively, and regulate the voltage at the sending bus 4 to become 1.0 p.u.

The result of voltage and phase angle of the system with GUPFC is presented in Table 2. The power flows result have justified the capability of NR based on power and current injection mismatches in solving load flow considering GUPFC model in the network. All the obtained values are fulfilling the specific control requirements of power flow that can be proven by calculating the power flow between lines 4–6 and 4–7 by using the obtained voltage and phase angle of the related buses.

The variation of the injected currents at the sending bus 4 and auxiliary buses 6, 7 and the total injected active power at sending bus addition against the iterations are presented in Fig. 6*a*. From this figure, it can be observed that the injected values at the terminals of GUPFC change rapidly for the first few iterations compared to the uncontrolled case. Consequently, the series and shunt GUPFC voltages reach to the final values at a few more iterations as shown in Fig. 6*b*.

5.2 Test case II

The IEEE 118-bus benchmark system is taken as a large-scale system. The IEEE-118 bus test system consists of 54 generators with 186 branches. The detail system data has been presented in [35]. The location of the GUPFC has been determined as in the literature [33]. The GUPFC is placed on lines 45-44 and 45-46. The main objective of adding the GUPFC is to control the complex powers flow of these lines and voltage magnitude at sending bus. Where, the specified power flow of line 45-44 is $40 + j7$ MVA and for line 45-46 is $-50 - j7$ MVA and the voltage magnitude of bus no. 45 is 1.00 p.u.

To verify the ability of the GUPFC model for steady-state operation at different specified power flows, various specified values of complex power flow through these lines and voltage magnitude at bus 45 are used and presented in Table 3. Case A, is considered the base case as given in [33]. However, the selected specified powers flow through transmission lines are within their accepted limits as given in motor.ece.iit.edu/data/SCUC_118test.xls [36]. The final values of injected power and currents at sending and auxiliary buses are presented in Table 4, also the shunt and series GUPFC voltage parameters are presented in the same Table 4.

5.3 Test case III: determination the operating constraints of GUPFC

The IEEE 30-bus test system is used to verify the developed handling strategies of operating constraints for GUPFC. The working range of

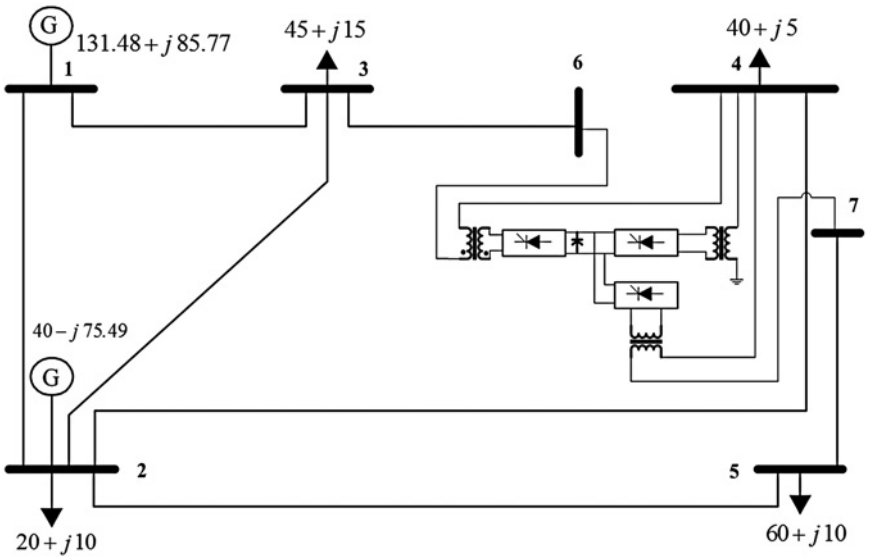

Fig. 5 *5-Bus test system including a GUPFC*

Table 2 Voltages of 5- bus test system with GUPFC

Nodal voltage	System bus					Auxiliary buses		GUPFC parameters		
	1	2	3	4	5	6	7	V_1^{se}	V_2^{se}	V^{sh}
magnitude, p.u.	1.060	1.000	1.0233	1.0000	0.9870	1.0298	1.0293	0.038	0.071	0.938
phase angle, deg.	0.000	1.764	1.3230	4.1531	0.3620	2.1056	5.4892	22.090	67.334	4.113

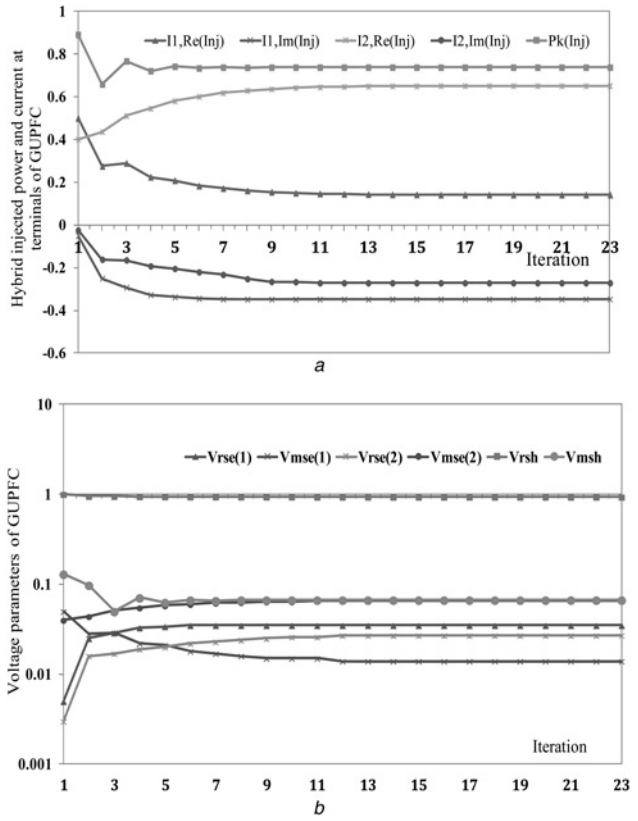

Fig. 6 *Convergence characteristics of developed GUPFC model in HPCIM for 5-bus test system*

a Convergence characteristics of HPCIM with a GUPFC
b Convergence characteristics of series and shunt GUPFC voltages

series injected voltages is (0.001–0.2) and (0.9–1.1) for the shunt injected voltages. The detail system data has been presented in [35]. There are two GUPFCs are connected in the system, whereas the locations and the selected specified values for GUPFCs are determined as in [33]. The shunt converter of first GUPFC is connected at bus 12 and the series converters are connected between buses 12–15 and 12–16. The set values of the specified voltage is 1 p.u. and the specified powers flow in lines 12–15 and 12–16 are 25 MW + j5 Mvar and 10 MW + j2 Mvar, respectively. The shunt converter of second GUPFC is connected at bus 10 and the series converters are connected between buses 10–21 and 10–22. The set values of the specified voltage is 1 p.u. and the specified powers flow in lines 10–21 and 10–22 are 10 MW + j6 Mvar and 12 MW + j4 Mvar, respectively, which are within their operating limits [37, 38]. Case (a) in Table 5, shows the parameters of the used GUPFCs without handling the operating constraints. Case (b) is similar to case (a) except that the maximum value of V_1^{se} of first GUPFC is limited to be 0.04 p.u. It was enforced by reducing P_1^{sp} to 20.1140 MW. Case (c) is similar to case (a) except that the maximum value of V_2^{se} is limited to be 0.04 p.u. It was enforced by reducing P_2^{sp} to 8.8920 MW. Case (d) is similar to case (a) except that the maximum value of V_1^{sh} is limited to be 0.950 p.u. It was enforced by relaxing V_1^{sp} to 0.980 p.u. Cases (e)–(g) are similar to case (a) except the maximum values of V_3^{se}, V_4^{se} and V_2^{sh} of second GUPFC are limited to be 0.0255, 0.0236 and 0.98 p.u, respectively. These constraints can be enforced by reducing P_3^{sp}, P_4^{sp}

Table 3 Different specified line flows for GUPFC on lines 45-44 and 45-46, IEEE 118-bus system

Case	P_{ih}^{sp}, MW	Q_{ih}^{sp}, Mvar	P_{jl}^{sp}, MW	Q_{ih}^{sp}, Mvar	V_k^{sp}, p.u	Connected lines
A	40	7	−50	−7	1.00	45/44(46)
B	5	−10	10	−5	1.00	
C	50	10	−60	−10.0	1.01	
D	20	5	−20	−2	1.02	

Table 4 Results of GUPFC model in IEEE 118-bus system at different values of specified line flow

Case	Injection currents at GUPFCs terminals					GUPFC parameters					
	I_1^{inj}, p.u		I_2^{inj}, p.u		P_k^{inj}, p.u	V_1^{se}		V_2^{se}		V^{sh}	
	Mag., p.u.	Ang., deg.	Mag., p.u.	Ang., deg.		Mag., p.u.	Ang., deg.	Mag., p.u.	Ang., deg.	Mag., p.u.	Ang., deg.
A	0.8957	−61.03	1.1681	178.85	1.0987	0.0896	28.96	0.1168	−91.14	1.0173	17.35
B	1.3879	158.31	1.7062	18.416	−1.7092	0.1387	−111.69	0.1706	108.42	1.0207	13.37
C	1.247	−33.55	1.6147	174.04	1.4775	0.1247	56.44	0.1615	−95.95	1.0260	17.42
D	0.8831	−140.0	0.38294	58.53	−0.2916	0.0883	−50.05	0.0383	148.53	1.0627	15.52

Table 5 Parameters of two GUPFCs embedded in IEEE 30-bus test system

	Case (a)	Case (b)	Case (c)	Case (d)	Case (e)	Case (f)	Case (g)	Case (h)	Case (i)
P_1^{sp}, MW	25	20.1140	25	25	25	25	25	17.206	25
Q_1^{sp}, MVAR	5	5	5	5	5	5	5	5	5
P_2^{sp}, MW	10	10	8.8920	10	10	10	10	10	7.81
Q_2^{sp}, MVAR	2	2	2	2	2	2	2	2	2
V_1^{sp}, p.u.	1	1	1	0.9800	1	1	1	1	1
P_3^{sp}, MW	10	10	10	10	9.7650	10	10	10	10
Q_3^{sp}, MVAR	6	6	6	6	6	6	6	6	6
P_4^{sp}, MW	12	12	12	12	12	10.3860	12	12	12
Q_4^{sp}, MVAR	4	4	4	4	4	4	4	4	4
V_2^{sp}, p.u.	1	1	1	1	1	1	0.9896	1	1
V_1^{se}, p.u.	0.0674 ∠62.56	0.0400 ∠66.16	0.0656 ∠62.41	0.0680 ∠53.29	0.0672 ∠62.66	0.0661 ∠63.23	0.0685 ∠66.09	0.0238 ∠73.23	0.0638 ∠62.26
I_{ih1}^{sp}, p.u.	0.2525	0.2071	0.2525	0.2548	0.2525	0.2528	0.2535	0.1800	0.2526
P_1^{se}, MW	0.0618	−0.0741	0.0648	0.3412	0.0583	0.0378	−0.0437	−0.1110	0.0675
V_2^{se}, p.u.	0.0505 ∠58.34	0.0427 ∠55.22	0.0400 ∠56.77	0.0558 ∠36.79	0.0510 ∠58.50	0.0535 ∠59.35	0.0516 ∠70.31	0.0380 ∠52.67	0.0298 ∠54.33
I_{jl1}^{sp}, p.u.	0.1007	0.1007	0.0902	0.1007	0.1007	0.1007	0.1018	0.1007	0.0800
P_2^{se}, MW	0.0545	0.0678	0.0374	0.2604	0.0538	0.0496	−0.0525	0.0764	0.0261
V_1^{sh}, p.u.	0.9807 ∠−16.39	0.9804 ∠−16.11	0.9805 ∠−16.27	0.9500 ∠−16.27	0.9807 ∠−16.39	0.9808 ∠−16.4	0.9817 ∠−16.47	0.9802 ∠−15.94	0.9804 ∠−16.16
I_1^{sh}, p.u.	0.1933	0.1960	0.1945	0.3000	0.1932	0.1924	0.1832	0.1981	0.1958
P_1^{sh}, MW	−0.1163	0.0063	−0.1022	−0.6017	−0.1121	−0.0873	0.0963	0.0347	−0.0937
Q_1^{sh}, MVAR	−19.3339	−19.600	−19.4506	−29.393	−19.3197	−19.237	−18.315	−19.81	−19.58
V_3^{se}, p.u.	0.0259 ∠133.60	0.0277 ∠144.34	0.0270 ∠130.17	0.0324 ∠138.22	0.0255 ∠138.76	0.0269 ∠161.27	0.0193 ∠124.76	0.0294 ∠149.95	0.0283 ∠127.06
I_{ih2}^{sp}, p.u.	0.1200	0.1205	0.1201	0.1209	0.1181	0.1206	0.1204	0.1208	0.1201
P_4^{se}, MW	−0.3108	−0.3274	−0.3242	−0.3906	−0.2999	−0.2852	−0.2297	−0.3391	−0.3377
V_4^{se}, p.u.	0.0307 ∠104.96	0.0298 ∠114.76	0.0324 ∠103.38	0.0355 ∠113.51	0.0296 ∠107.75	0.0236 ∠138.10	0.0268 ∠92.20	0.0298 ∠120.94	0.0342 ∠101.99
I_{jl2}^{sp}, p.u.	0.1290	0.1295	0.1290	0.1299	0.1291	0.1142	0.1294	0.1298	0.1290
P_5^{se}, MW	−0.2963	−0.3294	−0.3056	−0.3873	−0.2982	−0.2690	−0.2025	−0.3511	−0.3150
V_2^{sh}, p.u.	0.9975 ∠−15.86	0.9982 ∠−16.06	0.9977 ∠−15.97	0.9994 ∠−15.94	0.9976 ∠−15.8	0.9977 ∠−15.73	0.9800 ∠−15.83	0.9986 ∠−16.17	0.9978 ∠−16.08
I_2^{sh}, p.u.	0.0254	0.0193	0.0243	0.0096	0.0251	0.0235	0.0957	0.0155	0.0231
P_2^{sh}, MW	0.6071	0.6567	0.6299	0.7779	0.5980	0.5542	0.4322	0.6902	0.6527
Q_2^{sh}, MVAR	−2.4641	−1.8152	−2.3441	−0.5589	−2.4392	−2.2796	−9.4579	−1.3920	−2.21

and V_2^{sp} to be 9.7650 MW, 10.3860 MW and 0.9896 p.u, respectively. Case (h) is similar to case (a) except the maximum value of I_{ih}^{sp} is limited to be 0.1800 p.u., it was enforced by reducing P_1^{sp} to 17.206 MW. Case (i) is similar to case (a) except the maximum value of I_{jl}^{sp} is limited to be 0.08 p.u. It was enforced by reducing P_2^{sp} to 7.81 MW. However, if the transmission lines loadings or the apparent power of the GUPFC device is violated, it can be easily enforced by modifying the control specified values of GUPFC.

6 Conclusion

In this paper, a developed model of GUPFC in NR power and current mismatch load flow method has presented. In this model, power and currents are injected at the terminals of GUPFC depending on the required control values and updated buses voltage. The parameters of GUPFC can be updated during the iteration process. The impedances of the coupling transformers and the line charging susceptance are taken into account; while the original structure and symmetry of the admittance and Jacobian matrices can be unchanged. Based on this model, the incorporation of GUPFC in load flow become easy without changing in the basic computational algorithm, consequently, the complexities of the computer program codes are reduced. Furthermore, the problem when GUPFC is the only link between two sub networks is eliminated. The developed GUPFC model has been validated on standard IEEE test systems, excellent performance characteristics have been demonstrated.

7 References

1 Hingorani, N.G., Gyugyi, L.: 'Understanding FACTS – concepts and technology of flexible AC transmission systems' (IEEE Press, New York, 2000)

2 Zhang, X.-P., Rehtanz, C., Pal, B.C.: 'Flexible AC transmission systems: modelling and control' Springer Power Systems Series (Monograph, 2012)

3 Arrillag, J., Arnold, C.P., Harker, B.J.: 'Computer modelling of electrical power systems', ISBN: 9781118878286, doi: 10.1002/9781118878286, 2013
4 Stott, B., Alsac, O.: 'Fast decoupled load flow', *IEEE Trans. Power Appar. Syst.*, 1974, **PAS-93**, (3), pp. 859–869
5 Da Cost, V.M., Martins, N., Pereira, J.L.R.: 'Developments in the Newton-Raphson power flow formulation based on current injections', *IEEE Trans. Power Syst.*, 1999, **14**, (4), pp. 1320–1326
6 Da Cost, V.M., Martins, N., Pereira, J.L.R.: 'An augmented Newton-Raphson power flow formulation based on current injections', *Int. J. Electr. Power Energy Syst.*, 2001, **23**, pp. 305–312
7 Gyugyi, L., Schauder, C.D., Williams, S.L., *et al.*: 'The unified power flow controller: a new approach to power transmission control', *IEEE Trans. Power Deliv.*, 1995, **10**, (2), pp. 1085–1097
8 Nabavi-Niaki, A., Iravani, M.R.: 'Steady state and dynamic models of unified power flow controller (UPFC) for power system studies', *IEEE Trans. Power Syst.*, 1996, **11**, (4), pp. 1937–1943
9 Gyugyi, L., Schauder, C.D., Sen, K.K.: 'Static synchronous series compensator: a solid state approach to the series compensation of transmission lines', *IEEE Trans. Power Deliv.*, 1997, **12**, (1), pp. 406–417
10 Gyugyi, L., Sen, K.K., Schauder, C.D.: 'The interline power flow controller concept: a new approach to power flow management in transmission systems', *IEEE Trans. Power Deliv.*, 1999, **4**, (3), pp. 115–112
11 Fuerte-Esquivel, C.R., Acha, E.: 'Unified power flow controller: a critical comparison of Newton-Raphson UPFC algorithms in power flow studies', *IEE Proc., Gener. Transm. Distrib.*, 1997, **144**, (5), pp. 437–444
12 Fuerte-Esquivel, C.R., Acha, E., Ambriz-Perez, H.: 'A comprehensive Newton-Raphson UPFC model for the quadratic power flow solution of Practical power networks', *IEEE Trans. Power Syst.*, 2000, **15**, (1), pp. 102–109
13 Acha, E., Ambriz-Pérez, H., Fuerte-Esquivel, C.R., *et al.*: 'FACTS: modelling and simulation in power networks' (Wiley-Blackwell, 2004)
14 Zhang, X.-P.: 'Modelling of the interline power flow controller and the generalized unified power flow controller in Newton power flow', *IEE Proc., Gener. Transm. Distrib.*, 2003, **150**, (3), pp. 268–274
15 Nor, K.M., Mokhlis, H., Gani, T.A.: 'Reusability techniques in load-flow analysis computer program', *IEEE Trans. Power Syst.*, 2004, **19**, (4), pp. 1754–1762
16 Bhowmick, S., Das, B., Kumar, N.: 'An advanced IPFC model to reuse newton power flow codes', *IEEE Trans. Power Syst.*, 2009, **24**, (2), pp. 525–532
17 Bhowmick, S., Das, B., Kumar, N.: 'An indirect UPFC model to enhance reusability of newton power flow code', *IEEE Trans. Power Deliv.*, 2008, **23**, (4), pp. 2079–2088
18 Liu, J.Y., Song, Y.H., Mehta, P.A.: 'Strategies for handling UPFC constraints in steady-state power flow and voltage control', *IEEE Trans. Power Syst.*, 2000, **15**, (2), pp. 566–571
19 Zhang, X.-P.: 'Advanced modeling of the multi control functional static synchronous series compensator (SSSC) in Newton power flow', *IEEE Trans. Power Syst.*, 2003, **18**, (4), pp. 1410–1416
20 Zhang, Y., Zhang, Y.: 'A novel power injection model of embedded SSSC with mulit-control modes for power flow analysis inclusive of practical constraints', *Electr. Power Syst. Res.* , 2006, **76**, pp. 374–381
21 Zhang, Y., Zhang, Y., Chen, C.: 'A novel power injection model of IPFC for power flow analysis inclusive of practical constraints', *IEEE Trans. Power Syst.*, 2006, **21**, (4), pp. 1550–1556
22 Garcia, P.A., Pereira, J.L.R., Carneiro, S., *et al.*: 'Three-phase power flow calculations using the current injection method', *IEEE Trans. Power Syst.*, 2000, **21 15**, (2), pp. 508–514
23 Mayordomo, J.G., Izzeddine, M., Martínez, S., *et al.*: 'Compact and flexible three-phase power flow based on a full Newton formulation', *IEE Proc., Gener. Transm. Distrib.*, 2002, **149**, (2), pp. 225–232
24 Garcia, P.A.N., Pereira, J.L.R., Carneiro, S., *et al.*: 'Improvements in the representation of PV buses on three-phase distribution power flow', *IEEE Trans. Power Deliv.*, 2004, **19**, (2), pp. 894–896
25 Kamel, S., Abdel-Akher, M., Jurado, F.: 'Improved NR current injection load flow using power mismatch representation of PV bus', *Int. J. Electr. Power Energy Syst.*, 2013, **53**, pp. 64–68
26 Kamel, S., Abdel-Akher, M., El-Nemr, M.: 'A new technique to improve voltage controlled nodes (PV nodes) in the current injection Newton-Raphson power-flow analysis'. 45th Universities Power Engineering Conf. (UPEC 2010), Cardiff, Waales, UK, September 2010, pp. 1–4
27 Abdel-Akher, M., Kamel, S., El-nemr, M.: 'Load-flow analysis using hybrid power-current injection mismatches', *Int. Rev. Model. Simul. (I.RE.MO.S.)*, 2011, **4**, pp. 2382–2391
28 Kamel, S., Abdel-Akher, M., Jurado, F., *et al.*: 'Modeling and analysis of voltage and power control devices in current injections load flow method', *Electr. Power Compon. Syst.*, 2013, **41**, pp. 324–344
29 Kamel, S., Jurado, F.: 'Power flow analysis with easy modelling of interline power flow controller', *Electr. Power Syst. Res.* , 2014, **108**, pp. 234–244
30 Kamel, S., Jurado, F., Mihalic, R.: 'Advanced modeling of center-node unified power flow controller in NR load flow algorithm', *Electr. Power Syst. Res.*, 2015, **121**, pp. 176–182
31 Kamel, S., Jurado, F., Chen, Z.: 'Power flow control for transmission networks with implicit modeling of static synchronous series compensator', *Int. J. Electric. Power Energy Syst.*, 2015, **64**, pp. 911–920
32 Kamel, S., Jurado, F., Peças Lopes, J.A.: 'Comparison of various UPFC models for power flow control', *Electr. Power Syst. Res.* , 2015, **121**, pp. 243–251
33 Zhang, X.-P., Handschin, E., Yao, M.: 'Modeling of the generalized unified power flow controller (GUPFC) in a nonlinear interior point OPF', *IEEE Trans. Power Syst.*, 2001, **16**, (3), pp. 367–373
34 Demmel, J.W., Eisenstat, S.C., Gilbert, J.R., *et al.*: 'A supernodal approach to sparse partial pivoting', *SIAM J. Matrix Anal. Appl.*, 1999, **20**, (3), pp. 720–755
35 IEEE test systems data. Available at http://www.ee.washington.edu/research/pstca/
36 Khodaei, A., Shahidehpour, M.: 'Security-constrained transmission switching with voltage constraints', *Int. J. Electric. Power Energy Syst.*, 2012, **35**, pp. 74–82
37 Alsac, O., Stott, B.: 'Optimal load flow with steady state security', *IEEE Trans. Power Appar. Syst.*, 1974, **PAS-93**, (3), pp. 745–751
38 Taher, S.A., Amooshahi, M.K.: 'New approach for optimal UPFC placement using hybrid immune algorithm in electric power systems', *Int. J. Electric. Power Energy Syst.*, 2012, **43**, pp. 899–909